

# Tracer transport during the Arctic stratospheric final warming based on a 33-year (1979–2011) tracer equivalent latitude simulation

Douglas R. Allen,<sup>1</sup> Anne R. Douglass,<sup>2</sup> Gerald E. Nedoluha,<sup>1</sup> and Lawrence Coy<sup>3</sup>

Received 4 April 2012; revised 21 May 2012; accepted 22 May 2012; published 20 June 2012.

[1] During the 2011 stratospheric final warming (SFW), a large anticyclone rapidly encompassed the pole, displacing the polar vortex and establishing strong summer easterlies. Tracer Equivalent Latitude (TrEL) maps indicate low latitude air was transported by the anticyclone into the summer polar vortex. MLS nitrous oxide was anomalously high throughout the following summer, confirming the TrEL results. A 33-year (1979–2011) TrEL simulation at 850 K potential temperature reveals a number of similar low-TrEL events, which are often, but not always, associated with Frozen-In Anticyclone (FrIAC) formation. The summertime TrEL values are highly correlated with zonal wind speed in the polar stratosphere following the SFW, suggesting that strong post-SFW circulation favors polar trapping of low-TrEL air. The 2011 event, classified as a large-scale FrIAC, was unusual in having the lowest TrEL values and the strongest easterly vortex within the past three decades. **Citation:** Allen, D. R., A. R. Douglass, G. E. Nedoluha, and L. Coy (2012), Tracer transport during the Arctic stratospheric final warming based on a 33-year (1979–2011) tracer equivalent latitude simulation, *Geophys. Res. Lett.*, 39, L12801, doi:10.1029/2012GL051930.

## 1. Introduction

[2] The seasonal cycle of the Arctic extratropical stratospheric circulation is characterized by a strong winter polar vortex with cyclonic (westerly) circulation about the pole, reversing during the stratospheric final warming (SFW) to a weaker summer polar vortex with anticyclonic (easterly) circulation. This winter-to-summer transition produces persistent spatial structures in long-lived gases (tracers) in the summer vortex [Hess, 1991]. There is significant interannual variability in the timing and dynamical characteristics of the SFW due to external and internal forcings on the atmospheric circulation [Waugh and Rong, 2002; Waugh and Polvani, 2010]. For example, composites of stratospheric zonal wind for late SFW years show a deceleration in January forced by planetary wave activity, followed by a slow wind reversal in April and early May driven primarily by diabatic heating; early SFW composites shows only one rapid wind

deceleration in March forced by vigorous planetary wave activity [Black *et al.*, 2006; Wei *et al.*, 2007]. Strong coupling between the SFW and the tropospheric circulation occurs in both hemispheres [Black and McDaniel, 2007a, 2007b], suggesting that understanding SFW events is an important component of the stratosphere-troposphere downward coupling [Baldwin and Dunkerton, 2001].

[3] The dynamical differences in SFW events should be reflected in trace gas distributions near the summer pole. In this study, we seek to determine the dynamical conditions that favor the poleward transport and trapping of low-latitude air in the summer vortex. Recent studies have confirmed that long-lived features with characteristics of low latitude origin are occasionally observed in the polar region. These so-called Frozen-In Anticyclones (FrIACs) occur when anticyclonic vortices move from low- to high-latitudes and become trapped in the developing summer easterly flow. The vortices decay over about a month, but the accompanying tracer anomalies persist much longer. FrIACs have been identified using trace gas observations in 2003, 2005, and 2007 [Allen *et al.*, 2011; Lahoz *et al.*, 2007; Manney *et al.*, 2006; Thiéblemont *et al.*, 2011]. Manney *et al.* [2006] also found FrIAC-like signatures in analyzed potential vorticity in 1982, 1994, 1997, and 2002, but there are no accompanying observations of long-lived chemical tracers during those years. Thiéblemont *et al.* [2011] found that FrIAC occurrence is more likely in years with no major winter sudden stratospheric warming and with tropical quasi-biennial oscillation easterly phase. Their analysis of the context of the three known FrIACs was limited to the 10-year period from 2000–2009. This study places FrIACs in the broader context of interannual tracer variability near the summer pole from 1979–2011, relating FrIAC occurrence to the tracer variability and the dynamics of the SFW.

[4] In the absence of a multi-decadal dataset for stratospheric tracers, we use a 33-year (1979–2011) Tracer Equivalent Latitude (TrEL) simulation as a surrogate for actual tracer data. This simulation is described in Section 2. In Section 3 we detail TrEL evolution during the 2011 SFW, which was marked by an unusually large area of low TrEL air near the summer pole. Section 4 places the 2011 results in the context of TrEL variations over the entire time series, and Section 5 provides a summary and discussion.

## 2. Tracer Equivalent Latitude

[5] TrEL has been used to produce realistic tracer fields for studies of stratospheric transport and mixing including calculation of effective diffusivity, reconstruction of ozone mini-holes, analysis of aircraft campaign data in the polar lower stratosphere, and examination of transport during the

<sup>1</sup>Remote Sensing Division, Naval Research Laboratory, Washington, D. C., USA.

<sup>2</sup>NASA Goddard Space Flight Center, Greenbelt, Maryland, USA.

<sup>3</sup>Space Science Division, Naval Research Laboratory, Washington, D. C., USA.

Corresponding author: D. R. Allen, Remote Sensing Division, Naval Research Laboratory, 4555 Overlook Ave. SW, Washington, DC 20375, USA. (douglas.allen@nrl.navy.mil)

This paper is not subject to U.S. copyright.  
Published in 2012 by the American Geophysical Union.

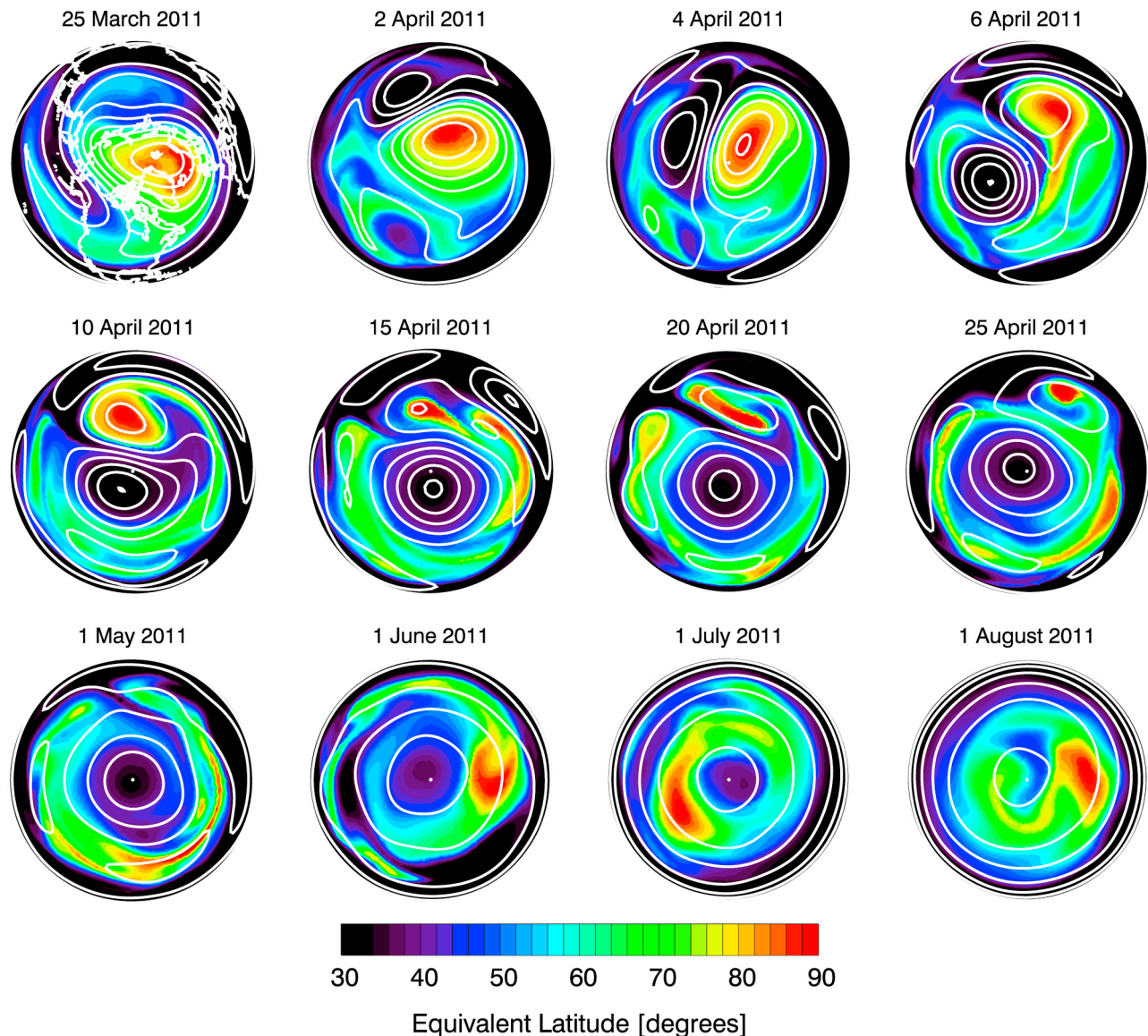


**Figure 1.** Northern Hemisphere TrEL at 850 K potential temperature ( $\sim 30$  km) for select days in March through August 2011. White contours are 850 K streamlines at constant intervals. High (low) TrEL is generally associated with cyclonic (anticyclonic) circulation. The maps use the orthographic projection with the Greenwich Meridian to the right (see continents on plot for 25 March 2011).

2002 Antarctic major warming [Allen and Nakamura, 2001, 2002, 2003; Allen *et al.*, 2003]; a complete description of TrEL calculation is provided in Allen and Nakamura [2003]. Briefly, TrEL is determined from the solution to the advection equation for a passive tracer on the sphere using a finite-volume technique on a triangular grid. The tracer is initialized on 1 January 1979 (12 Z) with mixing ratio equal to the sine of latitude. For this study we used 20,480 triangles (resolution  $\sim 240$  km) and isentropic advection at 850 K potential temperature forced by the streamfunction (i.e., non-divergent winds) derived from the Modern Era Retrospective-Analysis for Research and Applications (MERRA) reanalysis [Rienecker *et al.*, 2011]. The simulation runs through 2011, providing a continuous 33-year time series. The tracer mixing ratio is normalized each time step to global minimum/maximum values of  $-1/+1$  using a simple linear operator. The tracer mixing ratio is saved once per day (12 Z) and TrEL is calculated using  $TrEL(q) = \sin^{-1}(A(q)/2\pi a^2 - 1)$ , where  $A(q)$  is the area with

mixing ratio  $q$  less than a given value and  $a$  is the Earth's radius. Since the tracer is global, TrEL ranges from  $-90^\circ$  to  $+90^\circ$ . Since TrEL scales like latitude, it is useful for highlighting latitudinal transport. For example, low TrEL values at the North Pole indicate poleward transport and high TrEL values in the tropics indicate equatorward transport. Since TrEL is passive and driven by isentropic winds, it is not affected by interannual differences in photochemistry and diabatic transport. TrEL is therefore useful for studying interannual variability in isentropic transport.

### 3. Arctic Stratospheric Final Warming of 2011

[6] The 2011 Arctic winter vortex experienced more chemical ozone loss than any other year [Manney *et al.*, 2011]. This was due to unusually cold temperatures in the polar lower stratosphere in late-February and March, associated with weak planetary wave driving [Hurwitz *et al.*,

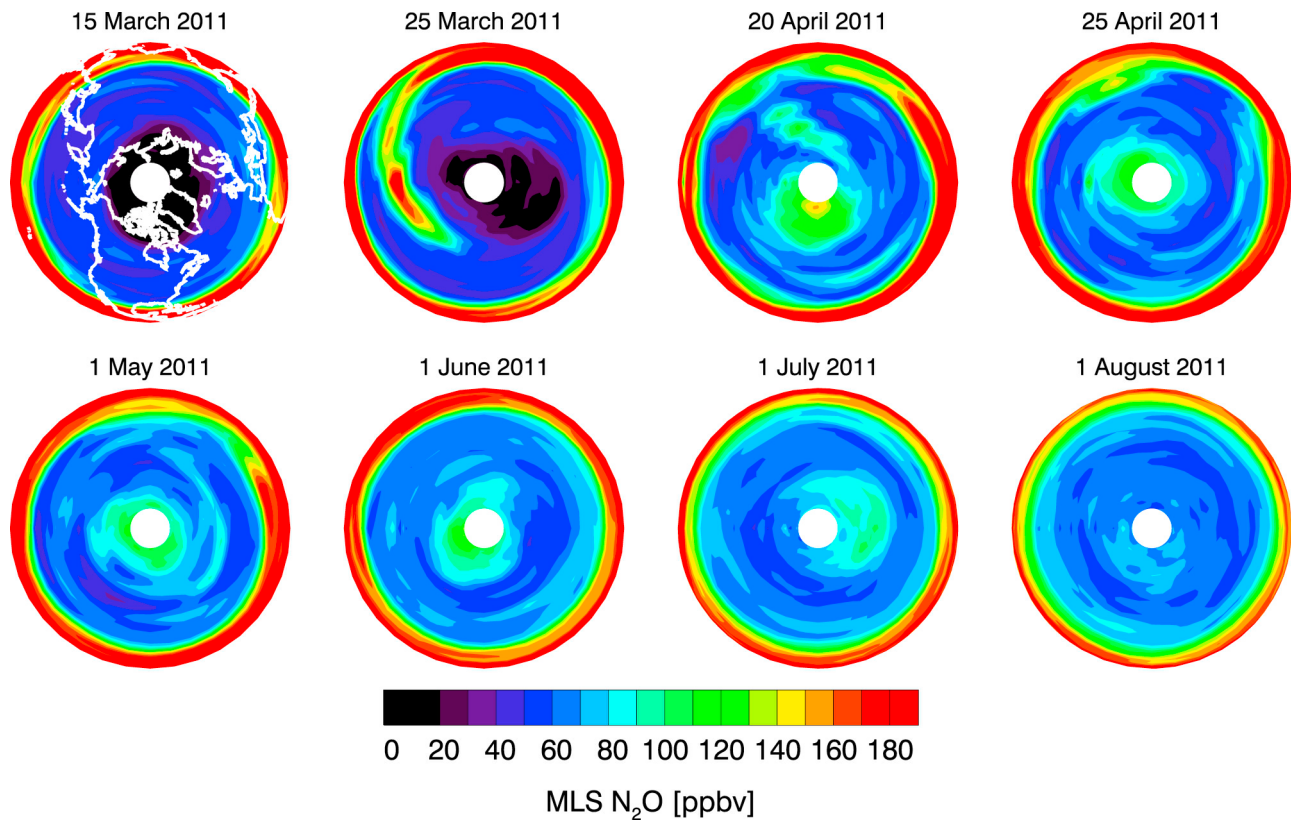


**Figure 2.** Northern Hemisphere MLS  $\text{N}_2\text{O}$  at 850 K potential temperature for select days in March–August 2011. MLS data are gridded using linear interpolation to  $10^\circ$  longitude spacing at the nominally defined level 2 latitudes (approximately  $1.5^\circ$  spacing). Data are smoothed using a  $3 \times 3$  boxcar smoothing in longitude and latitude. Map orientation is the same as Figure 1.

2011]. Here we show that a strong SFW in 2011 produced large, rapid tracer transport from low to high latitudes in the middle stratosphere. Figure 1 shows hemispheric maps of TrEL and streamfunction at 850 K potential temperature in March through August 2011. On 25 March, the winter vortex is identified by closed streamlines and high TrEL centered slightly off the pole. On 2 April, an anticyclone is seen over northern Asia. This anticyclone moves eastward and poleward from 2–10 April, bringing with it low-TrEL air from the tropics. The winter vortex is pushed off the pole during this period and weakens considerably. By 15 April, the anticyclone is established over the pole, with low TrEL throughout. This situation resembles the FrIAC events of 2003 and 2005, in which an anticyclone moves poleward and is trapped in the summer easterly flow. In 2011, however, the anticyclone completely dominates the polar region. In addition, high-TrEL air previously defining the winter vortex has spread out into a complete ring surrounding the pole (see 20 and 25 April). This condition makes TrEL an ambiguous marker of instantaneous meridional position, since low TrEL air exists both near the pole and at low latitudes. TrEL rather indicates the integrated history of air motion accompanying the SFW. The low TrEL air persists in the polar region throughout the summer, dissipating in early August.

[7] The March–August 2011 TrEL results are confirmed in Figure 2 with maps of Aura Microwave Limb Sounder (MLS) version 2.2 nitrous oxide ( $\text{N}_2\text{O}$ ); see Lambert *et al.* [2007] for validation of this product. Low  $\text{N}_2\text{O}$  marks the

winter vortex on 15 March, while a tongue of high  $\text{N}_2\text{O}$  air moves poleward on 25 March. Unfortunately, Aura MLS experienced an anomaly and did not make measurements from 27 March–19 April, completely missing the 2011 SFW. However, by 20 April, high  $\text{N}_2\text{O}$  is observed over a large portion of the polar cap. The contrast between 25 March and 20 April shows more than doubling of the  $\text{N}_2\text{O}$  mixing ratios in the polar region. A ring of low  $\text{N}_2\text{O}$  is visible on 25 April surrounding the pole, consistent with the high TrEL ring in Figure 1. The high  $\text{N}_2\text{O}$  near the pole persists into August, four months after the SFW. This persistence of high- $\text{N}_2\text{O}$  is similar to the 2005 FrIAC, which was also observed in MLS data [Allen *et al.*, 2011], but the 2005  $\text{N}_2\text{O}$  anomaly was considerably smaller.

#### 4. Interannual Variability During the Arctic SFW (1979–2011)

[8] The time-series of TrEL averaged over the polar cap ( $80^\circ$ – $90^\circ\text{N}$ ) is provided in Figure 3a for 1979–2011. As expected, in 2011 (see green line), a transition from high ( $\sim 80^\circ$ ) to low ( $\sim 35^\circ$ ) TrEL occurs during the SFW in early April. TrEL slowly increases in May and June, followed by more rapid increase in July and August, with high TrEL values becoming re-established at the pole by the end of August. Note that in each year, high TrEL is re-established at the pole by August as the high TrEL air mixes back towards the pole during the summer vortex breakdown. This interannual re-setting of the high TrEL values at the pole is

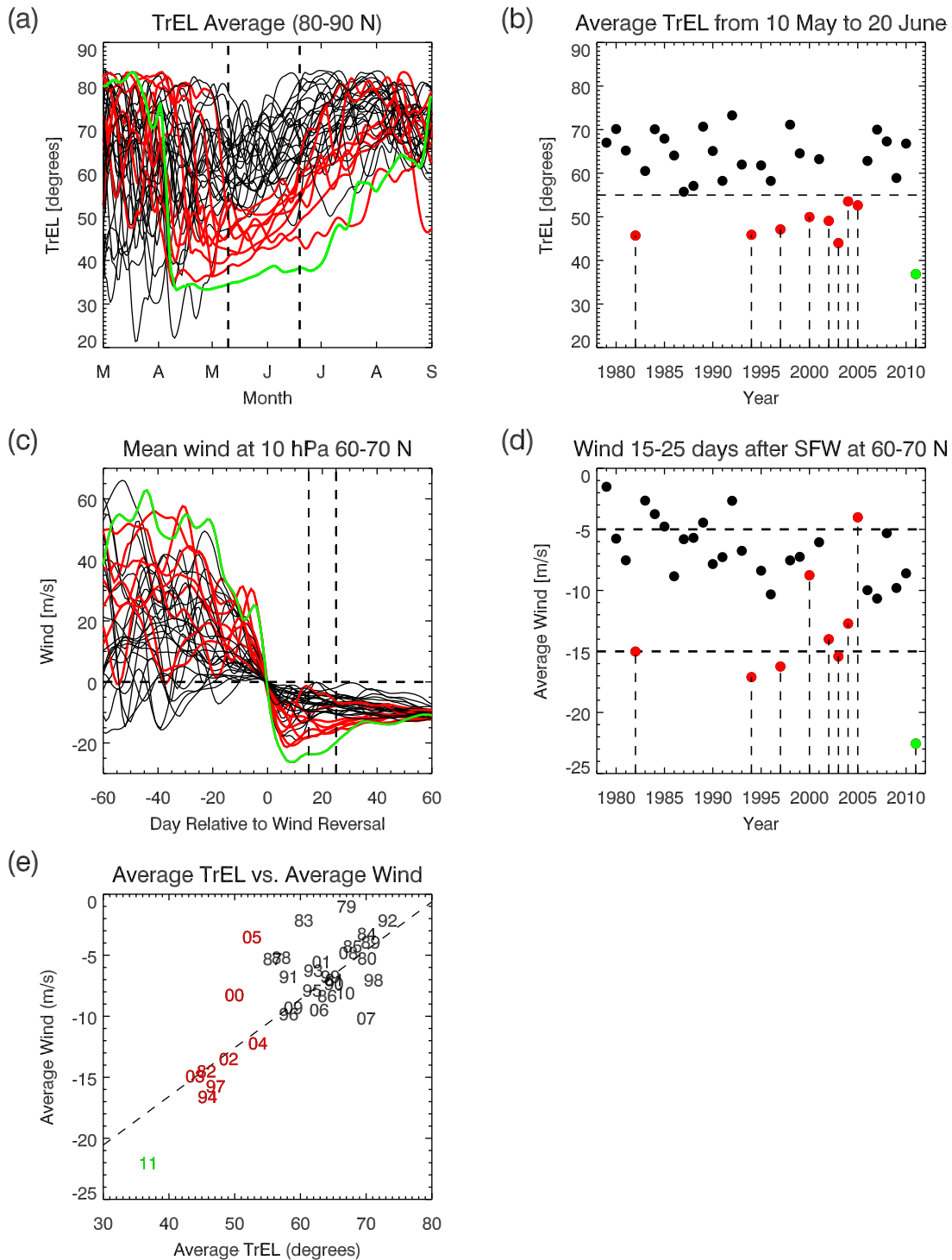


**Figure 3.** (a) TrEL at 850 K averaged from 80–90°N latitude for 1979–2011. Highlighted years in red (1982, 1994, 1997, 2000, 2002, 2003, 2004, and 2005) and green (2011) indicate TrEL values with a 10 May–20 June average of less than 55°. (b) TrEL averaged from 80–90°N and 10 May–20 June. (c) Zonal mean zonal wind at 10 hPa, 60–70°N for 1979–2011. For each year a 5-day smoothing is applied to remove high frequency variations and the data are shifted relative to the day of final wind reversal (see text for details). (d) Average zonal wind at 10 hPa, 60–70°N for 15–25 days following the wind reversal. (e) Scatter plot of values from Figure 3b versus values from Figure 3d. Dashed line shows the linear least-squares fit.

necessary for TrEL to be a useful tracer for interannual simulations.

[9] The 2011 SFW was unusual in terms of the magnitude and persistence of the low TrEL, as compared with other years (see Figure 3a). While there is large interannual

variability in TrEL during the SFW, there are several years with similar evolution to 2011, with very low TrEL established at the pole, followed by a slow relaxation to high TrEL by the end of the summer. The TrEL values averaged from 10 May–20 June of each year are shown in Figure 3b,

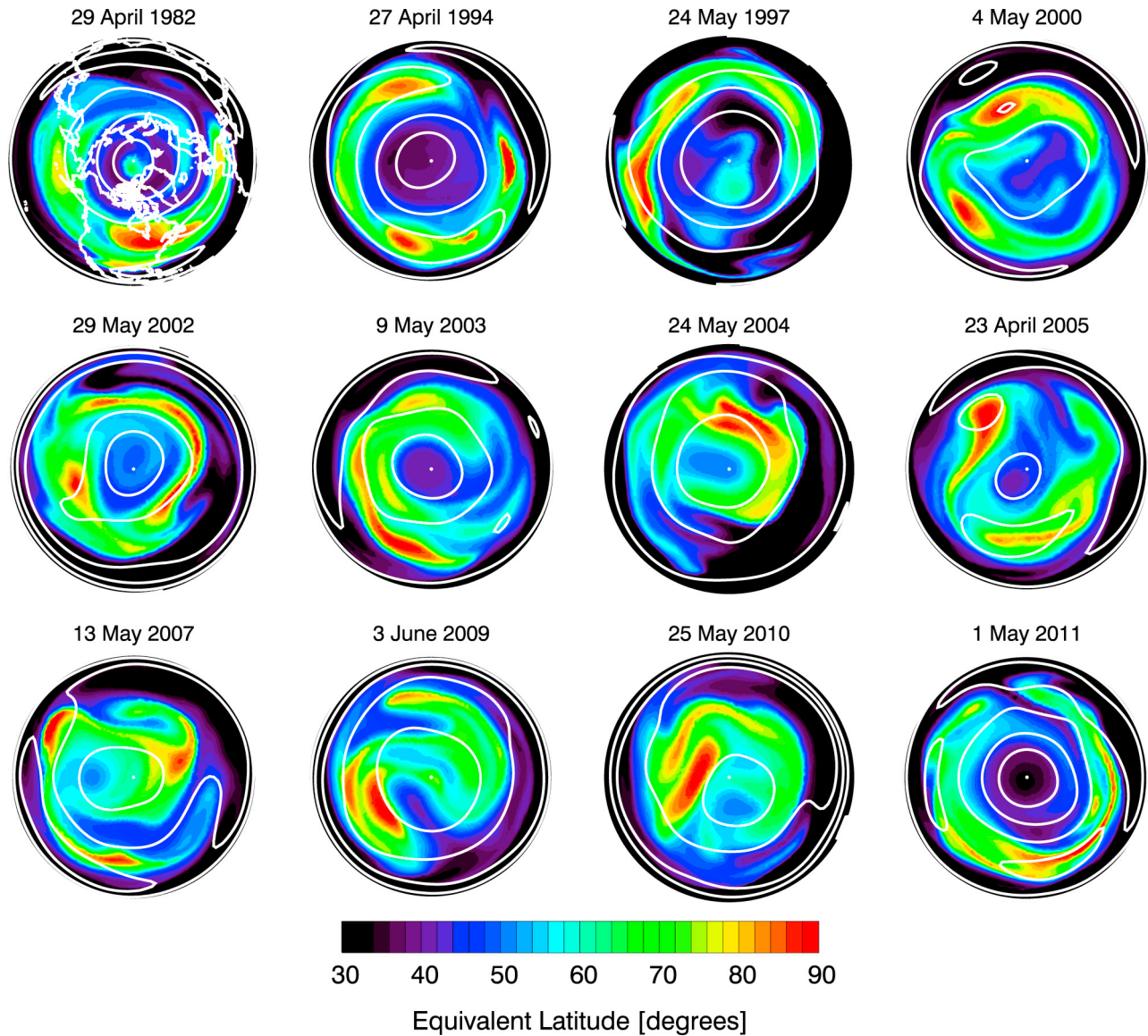


**Figure 4.** Northern Hemisphere TrEL at 850 K for the nine years highlighted in Figure 3 and, for comparison, three additional years (2007, 2009, and 2010). Each plot shows TrEL 25 days after the date of the SFW for that particular year. White contours are 850 K streamlines at constant intervals. Map orientation is the same as Figures 1 and 2.

with the nine lowest TrEL years (values less than  $55^\circ$ ) highlighted in red (1982, 1994, 1997, 2000, 2002, 2003, 2004, and 2005) and green (2011). With the exception of 2000 and 2004, these pre-2011 years were identified by Manney *et al.* [2006] as FrIAC years using potential vorticity. Note that in all years, some amount of low-TrEL air is enveloped into the summer vortex during the SFW. Our  $55^\circ$  TrEL cutoff, as well as the 80–90°N latitude averaging, are therefore somewhat arbitrary, and one cannot use these conditions to unambiguously identify FrIACs. Synoptic analyses, such as that done in Figure 1, are necessary to determine the origin of the observed low-TrEL air for each year. For example, in 2000, 2002 and 2004, the low-TrEL event formation is different from the previously studied FrIACs, with the anticyclone developing in the middle-latitudes rather than in the tropics. These years were therefore not identified as FrIAC years by Thiéblemont *et al.* [2011]. On the other hand, the 2007 FrIAC identified by

Thiéblemont *et al.* [2011] circled the pole at  $\sim 70^\circ\text{N}$ , and does not show up as unusual in our 80–90°N analysis.

[10] The TrEL interannual variability should be closely tied to the dynamical variability of the SFW. Thiéblemont *et al.* [2011] argued that years with abrupt and early final warmings favor FrIAC production, while years with slow transition during late SFWs are less likely to produce FrIACs. The synoptic analysis of Figure 1 shows that the 2011 SFW was marked by a large anticyclone that rapidly displaced the winter vortex. This results in rapid reversal of the zonal mean zonal wind at high latitudes; we therefore examine the time-evolution of the MERRA zonal mean zonal wind at 10 hPa, averaged from 60–70°N. We first identify the date of the SFW as when the zonal wind (smoothed with a 5-day running mean) at 10 hPa, 60–70°N turns negative for the last time until the subsequent winter vortex spin-up. We then time-shift the wind relative to the date of the SFW. Figure 3c shows these time-shifted winds,

and Figure 3d shows the average zonal wind 15–25 days after the SFW, with years identified with low TrEL values highlighted. Five of these years (1982, 1994, 1997, 2003, and 2011) are notable for having very strong easterlies (greater than  $\sim 15$  m/s) and very low average TrEL (less than  $\sim 50^\circ$ ). 2005 has rather weak easterlies for this time period; this year was unusual with the earliest SFW in the 33-year record (12 March) and is therefore considered an anomalous year. Strong, persistent easterlies associated with strong anticyclonic flow centered at the pole are necessary in order to trap the low-TrEL air that moved polewards during the SFW. The linear correlation coefficient between the average TrEL values in Figure 3b and the wind values in Figures 3d is very high (0.78), suggesting that this relationship is robust (see Figure 3e).

[11] TrEL maps for selected years are provided in Figure 4. Each map is a snapshot 25 days following the date of the SFW in that year. Maps for the low-TrEL years identified in Figure 3 generally show low TrEL values encompassing the closed streamlines surrounding the pole, while the highest TrEL air is elongated in the mid-latitudes. In other years (e.g., 2009, and 2010) the low TrEL air is off the pole and only fills a portion of the closed streamlines. The 2007 FrIAC is visible as a small low-TrEL feature over the date line at  $\sim 60^\circ$ N. Figure 4 provides a spectrum of post-SFW TrEL distributions and places the unusually large 2011 FrIAC in context.

## 5. Summary and Discussion

[12] The winter-to-summer transition in the Arctic polar middle stratosphere has been examined using a 33-year Tracer Equivalent Latitude simulation at 850 K driven by the MERRA reanalysis. In certain years, very low TrEL air is transported poleward and becomes trapped in the summer vortex. This is often, but not always, associated with a FrIAC. The 2011 large-scale FrIAC was the most significant in terms of the magnitude and persistence of low TrEL and strong easterlies following the SFW. The dynamics of these events resemble low-ozone pocket formation, in which low-latitude air is drawn into a developing anticyclone and isolated from surrounding air, resulting in chemical ozone loss [Harvey *et al.*, 2008, and references therein]. Low-ozone pockets disappear with the decay of the anticyclone; FrIACs, however, become fixed into the summer circulation and serve as the “seed” of the summertime easterly circulation. The synoptic analyses presented in Figure 1 show that zonal wind reversal is caused by the anticyclone displacing the winter polar vortex, a common feature for all identified FrIAC years.

[13] The dynamics of SFWs are sensitive to the timing of the vortex breakup [Thiéblemont *et al.*, 2011]. In the composite analysis of Wei *et al.* [2007], early breakup years showed rapid wind reversal, with wind speed dropping from 30 m/s to  $-10$  m/s over a month; this is similar to what occurred in 1982, 1994, 1997, 2003, and 2011. In late breakup years, an early vortex deceleration due to planetary wave activity results in a weaker polar vortex that transitions more gradually to summer conditions. These dynamical differences result in different meridional transport, with early breakup years favoring poleward transport of low TrEL that becomes trapped near the pole. The breakup dates according to our analysis at 850 K for the five large-scale

FrIAC years were 4 April 1982, 2 April 1994, 14 April 2003, 29 April 1997, and 6 April 2011. Four of these years are early breakups (note that the mean breakup date according to our criteria is 15 April). 1997 had an unusually strong, persistent cold vortex [Coy *et al.*, 1997] that broke up quickly in late April. Further planned studies with multi-decade chemistry climate model simulations will examine whether the modeled climatology of tracer distributions during SFWs agrees with the observed interannual variability. This approach will complement the analysis of mid-winter major stratospheric warming climatologies that have been used to test the interannual dynamical variability in general circulation models [Charlton and Polvani, 2007; Charlton *et al.*, 2007].

[14] **Acknowledgments.** This work was supported by a subcontract by the NASA ACPMAP Program (NNHH09ZDA001N). Work at NRL is sponsored by the Office of Naval Research. We would like to thank the two anonymous reviewers for helpful comments and suggestions.

[15] The Editor thanks the two anonymous reviewers for assisting in the evaluation of this paper.

## References

- Allen, D. R., and N. Nakamura (2001), A seasonal climatology of effective diffusivity in the stratosphere, *J. Geophys. Res.*, *106*(D8), 7917–7935, doi:10.1029/2000JD900717.
- Allen, D. R., and N. Nakamura (2002), Dynamical reconstruction of the record low column ozone over Europe on 30 November 1999, *Geophys. Res. Lett.*, *29*(9), 1362, doi:10.1029/2002GL014935.
- Allen, D. R., and N. Nakamura (2003), Tracer equivalent latitude: A diagnostic tool for isentropic transport studies, *J. Atmos. Sci.*, *60*(2), 287–304, doi:10.1175/1520-0469(2003)060<0287:TELADT>2.0.CO;2.
- Allen, D. R., R. M. Bevilacqua, G. E. Nedoluha, C. E. Randall, and G. L. Manney (2003), Unusual stratospheric transport and mixing during the 2002 Antarctic winter, *Geophys. Res. Lett.*, *30*(12), 1599, doi:10.1029/2003GL017117.
- Allen, D. R., A. R. Douglass, G. L. Manney, S. E. Strahan, J. C. Krosschell, J. V. Trueblood, J. E. Nielsen, S. Pawson, and Z. Zhu (2011), Modeling the frozen-in anticyclone in the 2005 Arctic summer stratosphere, *Atmos. Chem. Phys.*, *11*(9), 4557–4576, doi:10.5194/acp-11-4557-2011.
- Baldwin, M. P., and T. J. Dunkerton (2001), Stratospheric harbingers of anomalous weather regimes, *Science*, *294*(5542), 581–584, doi:10.1126/science.1063315.
- Black, R. X., and B. A. McDaniel (2007a), The dynamics of Northern Hemisphere stratospheric final warming events, *J. Atmos. Sci.*, *64*(8), 2932–2946, doi:10.1175/JAS3981.1.
- Black, R. X., and B. A. McDaniel (2007b), Interannual variability in the Southern Hemisphere circulation organized by stratospheric final warming events, *J. Atmos. Sci.*, *64*(8), 2968–2974, doi:10.1175/JAS3979.1.
- Black, R. X., B. A. McDaniel, and W. A. Robinson (2006), Stratosphere-troposphere coupling during spring onset, *J. Clim.*, *19*(19), 4891–4901, doi:10.1175/JCLI3907.1.
- Charlton, A. J., and L. M. Polvani (2007), A new look at stratospheric sudden warmings. Part I: Climatology and modeling benchmarks, *J. Clim.*, *20*(3), 449–469, doi:10.1175/JCLI3996.1.
- Charlton, A. J., L. M. Polvani, J. Perlwitz, F. Sassi, E. Manzini, K. Shibata, S. Pawson, J. E. Nielsen, and D. Rind (2007), A new look at stratospheric sudden warmings. Part II: Evaluation of numerical model simulations, *J. Clim.*, *20*(3), 470–488, doi:10.1175/JCLI3994.1.
- Coy, L., E. R. Nash, and P. A. Newman (1997), Meteorology of the polar vortex: Spring 1997, *Geophys. Res. Lett.*, *24*(22), 2693–2696, doi:10.1029/97GL52832.
- Harvey, V. L., C. E. Randall, G. L. Manney, and C. S. Singleton (2008), Low-ozone pockets observed by EOS-MLS, *J. Geophys. Res.*, *113*, D17112, doi:10.1029/2007JD009181.
- Hess, P. G. (1991), Mixing processes following the final stratospheric warming, *J. Atmos. Sci.*, *48*(14), 1625–1641, doi:10.1175/1520-0469(1991)048<1625:MPFTFS>2.0.CO;2.
- Hurwitz, M. M., P. A. Newman, and C. I. Garfinkel (2011), The Arctic vortex in March 2011: A dynamical perspective, *Atmos. Chem. Phys.*, *11*(22), 11,447–11,453, doi:10.5194/acp-11-11447-2011.
- Lahoz, W. A., A. J. Geer, and Y. J. Orsolini (2007), Northern Hemisphere stratospheric summer from MIPAS observations, *Q. J. R. Meteorol. Soc.*, *133*(622), 197–211, doi:10.1002/qj.24.

- Lambert, A., et al. (2007), Validation of the Aura Microwave Limb Sounder middle atmosphere water vapor and nitrous oxide measurements, *J. Geophys. Res.*, *112*, D24S36, doi:10.1029/2007JD008724.
- Manney, G. L., N. J. Livesey, C. J. Jimenez, H. C. Pumphrey, M. L. Santee, I. A. MacKenzie, and J. W. Waters (2006), EOS Microwave Limb Sounder observations of “frozen-in” anticyclonic air in arctic summer, *Geophys. Res. Lett.*, *33*, L06810, doi:10.1029/2005GL025418.
- Manney, G. L., et al. (2011), Unprecedented Arctic ozone loss in 2011, *Nature*, *478*(7370), 469–475, doi:10.1038/nature10556.
- Rienecker, M. M., et al. (2011), MERRA: NASA’s Modern-Era Retrospective Analysis for Research and Applications, *J. Clim.*, *24*(14), 3624–3648, doi:10.1175/JCLI-D-11-00015.1.
- Thiéblemont, R., N. Huret, Y. J. Orsolini, A. Hauchecorne, and M. A. Drouin (2011), Frozen-in anticyclones occurring in polar Northern Hemisphere during springtime: Characterization, occurrence and link with quasi-biennial oscillation, *J. Geophys. Res.*, *116*, D20110, doi:10.1029/2011JD016042.
- Waugh, D. W., and L. M. Polvani (2010), Stratospheric polar vortices, in *The Stratosphere: Dynamics, Transport, and Chemistry, Geophys. Monogr. Ser.*, vol. 190, edited by L. M. Polvani, A. H. Sobel, and D. W. Waugh, pp. 43–57, AGU, Washington, D. C., doi:10.1029/2009GM000887.
- Waugh, D. W., and P. P. Rong (2002), Interannual variability in the decay of lower stratospheric Arctic vortices, *J. Meteorol. Soc. Jpn.*, *80*(4B), 997–1012, doi:10.2151/jmsj.80.997.
- Wei, K., W. Chen, and R. H. Huang (2007), Dynamical diagnosis of the breakup of the stratospheric polar vortex in the Northern Hemisphere, *Sci. China Ser. D*, *50*(9), 1369–1379, doi:10.1007/s11430-007-0100-2.